Transfer of ^{6}Li break-up fragments at ^{6}Li projectile energies far above the Coulomb barrier

B. Neumann, J. Buschmann,
H. Klewe-Nebenius, H. Rebel, H. J. Gils
Institut für Angewandte Kernphysik

Kernforschungszentrum Karlsruhe

KERNFORSCHUNGSZENTRUM KARLSRUHE

Institut für Angewandte Kernphysik

KfK 2819

TRANSFER OF ^{6}Li-BREAK-UP FRAGMENTS
AT ^{6}Li PROJECTILE ENERGIES
FAR ABOVE THE COULOMB BARRIER

B. Neumann, J. Buschmann, H. Klewe-Nebenius[+],
H. Rebel and H.J. Gils

[+] Institut für Radiochemie, Kernforschungszentrum Karlsruhe

ABSTRACT

Transfer of beam-velocity fragments has been experimentally investigated in ^{6}Li induced reactions on ^{208}Pb and ^{209}Bi in the energy range E_{Li}=60-156 MeV. The experimental techniques involve the observation of the target residues and measurements of the recoil ranges of heavy residual nuclei produced by charged particle bombardment. The determination of the recoil energy enables the discrimination of different reaction paths leading to the same residual nuclei. (^{6}Li,xn+p) excitation functions prove to be very similar to (α,(x-1)n) reactions at $E_\alpha \sim 2/3 \cdot E_{Li}$. The results present experimental evidence for a particular reaction type indicated in previous experiments: Dissociation of the ^{6}Li projectile with capture of the beam-velocity alpha particle indicating an (α,xn) reaction ("internal break-up").

Transfer von ^{6}Li-Aufbruch-Fragmenten bei ^{6}Li-Projektil-Energien weit über der Coulomb-Barriere

ZUSAMMENFASSUNG

Prozesse, bei denen Dissoziationsprodukte des Projektils in ^{6}Li induzierten Kernreaktionen an ^{208}Pb und ^{209}Bi transferiert werden, wurden experimentell im Energiebereich E_{Li} = 60-156 MeV untersucht. Die Experimente basieren auf der Beobachtung schwerer Restkerne, die bei der ^{6}Li-Bestrahlung der Targets erzeugt werden, sowie auf Messungen der Reichweite der Rückstoßkerne in Kohlenstoff-Folien. Die Bestimmung der Rückstoßenergie ermöglicht eine Unterscheidung verschiedener möglicher Reaktionswege, die zum gleichen Endkern führen. Die Anregungsfunktionen für (^{6}Li,xn+p)-Reaktionen zeigen eine auffällige Ähnlichkeit mit (α,(x-1)n)-Reaktionen bei $E_\alpha \sim 2/3 \cdot E_{Li}$. Die Ergebnisse machen einen schon in früheren Experimenten angedeuteten Reaktionsmechanismus evident: ^{6}Li-Aufbruch mit Einfang eines Fragments, das eine (Fragment,xn)-Reaktion einleitet ("internal break-up").

1. INTRODUCTION

Nuclear reactions which are induced by ^{6}Li particles exhibit interesting features originating from the pronounced cluster structure of the ^{6}Li projectile. The dominating reaction channel is the break-up of ^{6}Li into various different fragments, in particular into an alpha-particle and a deuteron. At beam energies near the Coulomb barrier many kinematically incomplete experiments[1,2] and kinematically complete correlation studies[3,4] have investigated the dissociation of the ^{6}Li nucleus in the field of the target nucleus. The sequential break-up via inelastic scattering to resonant states (particularly to the 3^+_1 state of ^{6}Li at E_x = 2.18 MeV), nonsequential break-up and inelastic break-up processes through transfer and pick-up reactions (^{6}Li → ^{5}Li → α+p) and ^{6}Li → ^{8}Be α +α) have been found to play roles. With increasing ^{6}Li energy a transition from pure Coulomb break-up to the break-up in the nuclear field is expected[5]. Simultaneously the reaction mechanism dominated by the sequential break-up near the Coulomb barrier changes to immediate fragmentation of the 6Li nucleus into continuum states. Fig. 1 displays energy spectra of light outgoing particles when bombarding ^{208}Pb by 156 MeV ^{6}Li ions. The broad bumps centered at the beam-velocity reflect the importance of the break-up channels. At higher energies, in addition to the familiar (α + d) component the dissociation of ^{6}Li → ^{3}He + t (Q=-15.8 MeV) is clearly observed. Three particle break-up processes ^{6}Li → p + n + α and secondary deuteron break-up may explain the proton bump observed at E $\sim$ 1/6 E_{Li}. Similarly the triton spectrum may have a component from the secondary break-up of excited α-particles. Systematic investigations of such (inclusive type) continuum particle spectra induced by bombardment with 156 MeV ^{6}Li ions, measurements of the angular and A-dependence of the "bump" cross sections and studies of various contributing components will be reported elsewhere[6].

The extremely high break-up probability - in fact with cross sections σ_{Diss} as high as the elastic cross section - suggests that the dissociation processes strongly interfere with other reaction channels and may lead to peculiar types of reaction mechanisms. When bombarding Au and Ir targets
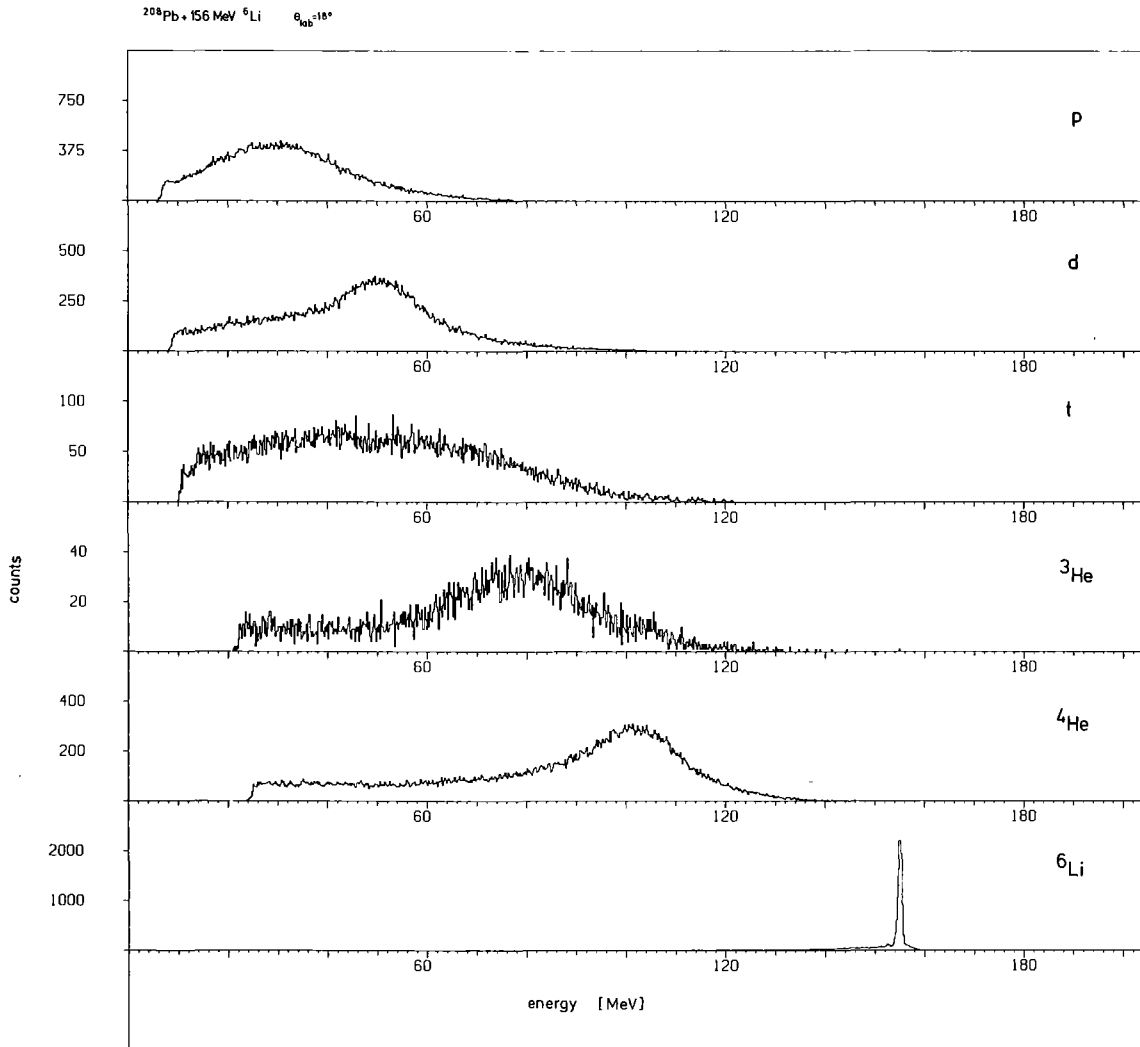
$^{208}Pb + 156\,MeV\ ^6Li \quad \theta_{lab} = 18°$

Fig. 1: Energy spectra of outgoing light charged particles
when bombarding ^{208}Pb by 156 MeV ^6Li ions.

with 48 - 156 MeV ^6Li ions and measuring excitation functions Kropp et al.[7] noticed a conspicuous enhancement of the cross sections for charged particle exit channels with respect to merely neutron emitting reactions. This observation has been attributed to the ^6Li break-up with a transfer of one of the break-up fragments into the target nucleus, forming a compound nucleus in the preequilibrium stage while the other fragment plays more or less the role of a spectator. Cross section measurements for (^6Li,xn+yp) reactions induced by 50-100 MeV ^6Li ions on Pd[8] and on rare earth[9] targets supported the existence of such an interesting reaction mechanism involving specific aspects of inelastic break-up processes and multinucleon transfer reactions into highly excited states. Recently[10], particle-gamma-coincidence experiments with 75 MeV ^6Li ions on ^{197}Au have definitively confirmed this particular reaction channel showing that at this energy a part of 13 % of beam-velocity particles is associated with ^6Li-fragment capture reactions.

In the present paper we report on detailed experimental studies[+] of break-up fragment capture reactions considering the case $^6Li + ^{208}Pb$ in the energy range E_{Li} = 60-156 MeV. The experiments are based on the observation of the target residues, in particular of ^{211m}Po, and on measurements of the recoil energies of residual nuclei produced by the charged particle bombardment. The results provide further evidence for cluster transfer reactions into highly excited nuclear states and reveal the relative importance of such processes in the case of ^6Li induced reactions. Moreover, by measuring $(^6Li,xn+yp)$ excitation functions and by comparing with alpha particle induced reactions it turns out that at ^6Li energies well above the Coulomb barrier $(^6Li,xn+p)$ reactions can be regarded to be essentially $(\alpha,(x-1)n)$ reactions at alpha-particle energies $E_\alpha \sim 2/3 \ E_{Li}$ with a neutron-proton pair as spectator.

2. PRINCIPLES AND PROCEDURES

There are different reaction paths leading to the same residual nucleus after charged particle irradiation of the target. Considering the case: ^6Li on ^{208}Pb the residual nucleus ^{211m}Po may be produced by the reaction

$$(^6Li + ^{208}Pb) \rightarrow ^{214}At^* \rightarrow ^{211m}Po + 2n + p \qquad (I)$$
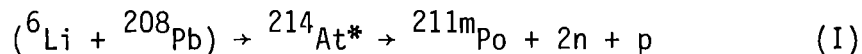
This compound nucleus formation followed by the emission of two neutrons and one proton competes with the mechanism under consideration: *break-up of the ^6Li projectile followed by capture of the beam-velocity alpha-particle*

$$^6Li \begin{cases} (\alpha + ^{208}Pb) \rightarrow ^{212}Po^* \rightarrow ^{211m}Po + n \\ d\text{-spectator} \end{cases} \qquad (II)$$
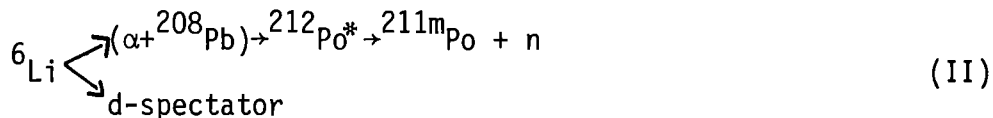
[+] Some results have already been published in ref. 11.

The multi-nucleon transfer reaction (II) fulfills roughly the kinematically founded optimum Q-value criterion (closest approach distance matching)[12] which has been shown to govern the transfer probabilities in heavy ion reactions at lower energies. Possible transfer processes leading to isolated low-lying, quasi-stable states (of the same final nucleus)

$$^{6}Li + ^{208}Pb \rightarrow ^{211m}Po + t \qquad\qquad (III)$$
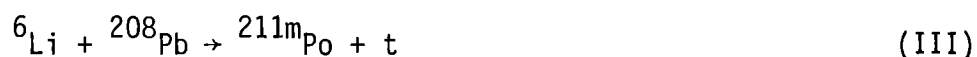
are outside the Q-window and are expected to have small cross-sections since the Q-value criterion persists to some extent at increased bombarding energies[13]. It should also be noted that there is certainly a change in character of the transfer reactions between (II) and (III). While the direct transfer to low-lying states of the final nucleus (type III) is assumed to involve only a few degrees of freedom of the colliding nuclei the multi-nucleon transfer of beam-velocity fragments is expected to proceed predominantly by the compound nucleus mechanism. Emphasizing this differnence and indicating the origin of the multi-nucleon transfer (II) we suggest to denote type II "*internal break-up*".

Excluding explicitely gamma-decay from neutron unstable states of $^{211}Po^{*}$ (populated via beam velocity ^{3}He particles[+]) ^{211m}Po production will occur mainly by the two reaction ways (I) and (II). The experimental discrimination between these processes is possible due to different recoil energies of the residual nucleus ^{211m}Po. For E_{Li} = 156 MeV the fusioned nucleus (type I) recoils with E_R = 4.4 MeV whereas for the reaction II induced by the beam-velocity α-particles ($E_\alpha \sim$ 104 MeV) $E_R \sim$ 1.9 MeV is calculated when assuming the recoils and the spectator deuterons to be emitted mainly in forward direction. For the direct branch (III) E_R is estimated 0.7 MeV assuming the light particles to escape in forward direction and excitation energies of the product nucleus E_x<10 MeV. Even if we take into account that these values are not sharp for the residual nucleus finally observed (due to evaporation of light particles, in case I and II, angular distribution of the recoiling nucleus

---

[+]
    One component indicated in the triton spectrum of fig. 1 might
    be associated with such a transfer.

and energy spread of the fragments) the differences in E_R are suf-ficiently separated for a clear discrimination.

In our experiments the recoiling nuclei leaving the target have been catched in carbon foils of various thicknesses and identified by the alpha decay (decay energy E_α and half life $T_{1/2}$). The implantation depths of the nuclei recoiling into the catcher foil depend on the location of the nuclear reaction in the target. When looking at particular product nuclide with definite recoil energy the yield of implanted nuclei depends on the catcher thickness as schematically shown in fig. 2.
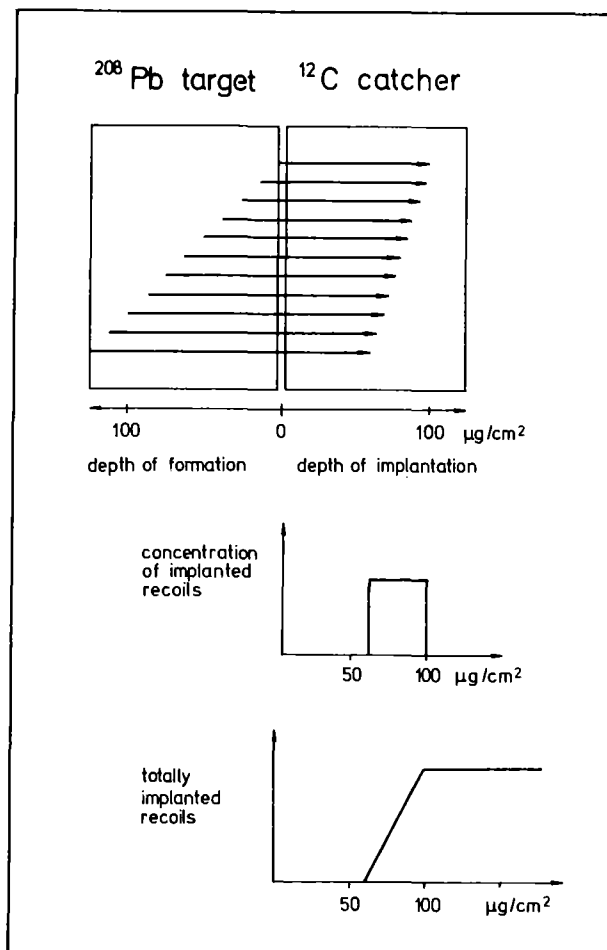

Fig. 2: Implantation depth of nuclei recoiling into a carbon catcher and corresponding yield of recoil nuclei (schematically).

For catcher thicknesses smaller than the range of the recoiling nuclei, only part of the nuclei leaving the target are stopped. When the catcher thickness exceeds the range corresponding to the recoil energy one will observe a constant yield since all recoils of the considered reaction component are stopped. The energy distribution of the transferred fragments as well as the angular distribution of the recoils will smear out the transition leading to an experimental uncertainty of the recoil energy of about 0.5 MeV.

An additional method for determining of the recoil energy is provided by the energy loss of the alpha particles emitted by the decaying residues and transversing the residual thickness of the catcher foils. The energy shifts of the alpha-lines due to self-absorption inform about the location of the recoil nuclei in the catcher. The experimental procedure requires a good energy resolution of the alpha spectrometer ($\sim$30 keV FWHM) and a precise energy calibration .

3. IRRADIATION AND ALPHA ACTIVITY MEASUREMENTS

The experimental technique used for the determination of the recoil energy is similar to the method applied by Bimbot et al.[15]. The irradiations were performed using the external beam of the Karlsruhe Isochronous Cyclotron providing 104 MeV alpha particles and 156 MeV ^{6}Li ions. For excitation function measurements the primary beam energy was stepwise degraded[17] by Be-sheets. The beam current, typically 400 nA for alpha particles and 15 nA for ^{6}Li, was measured by means of a Faraday cup behind the irradiation chamber. The thickness of the ^{208}Pb target was 150 μg/cm^2 on a 20 μg/cm^2 carbon backing. To produce the nuclide ^{211m}Po by alpha irradiation, a 360 mg/cm^2 thick Bi target,evaporated onto a 10 μm thick Al foil,was used.The targets were fixed with their backing looking upstream.The target and catcher thicknesses were determined by measuring the energy loss of ^{241}Am alpha particles(uncertainty $\pm$5%).The catcher foils were mounted on a pneumatically driven slider. Fig. 3 displays a schematic view of the experimental set-up. After irradiating the target during a few half-lives of the product nucleus under consideration, the beam has been switched off and the catcher was transported between a pair of opposite

mounted Si surface barrier detectors with an acceptance of 25 % of
4π. Each measuring cycle consisted of the irradiation period, the
recording period, and the transport period, forth and back. The timing was
performed by an automatic controller described in ref. 18.

After each run (5-6 hours) the catcher foil were changed in
order to avoid the accummulation of longer-lived alpha-activities.In
a pre-run the peaks in the alpha-particle spectra were identified
via the half-life by measuring in a multi-spektrum scaling procedure.
The uncertainty in the absorption curves (fig.6) is essentially due to the statisti-
cal errors of 10-30 % (considerably increasing for thin carbon catchers).
The evaluation of cross-sections implies the knowledge of the recoil
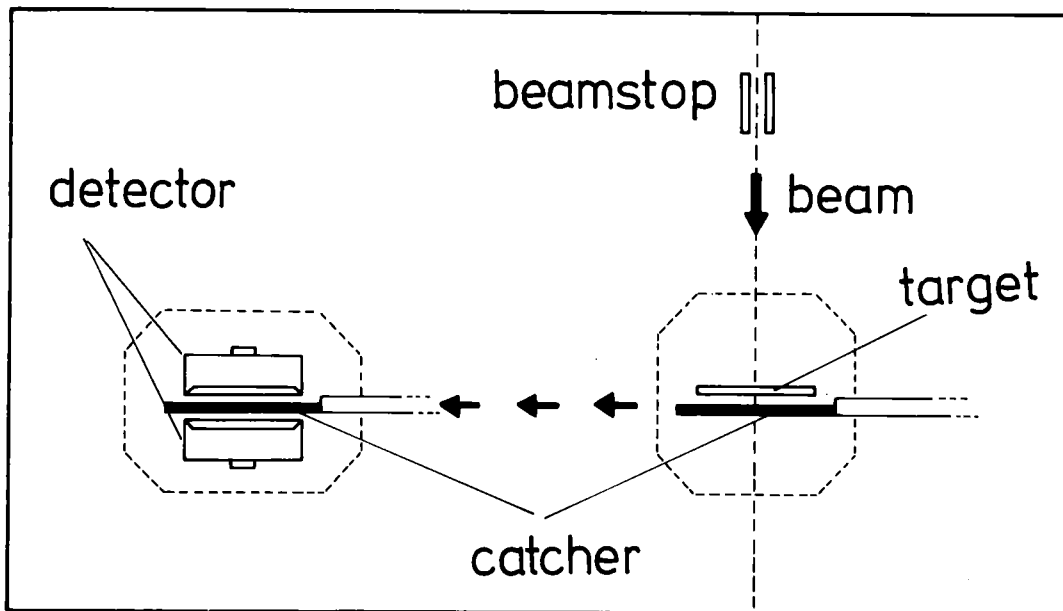catching efficiency. By mounting the target together with a thick

Fig. 3: Experimental set-up for measuring the recoil energy of alpha-
decaying residual nuclei with $T_{1/2} \geq 10$ sec.

catcher on the pneumatic driver the catching efficiency was experimentally determined to be nearly 100 %. Counting pile-up due to contributions from cycles before were corrected for.
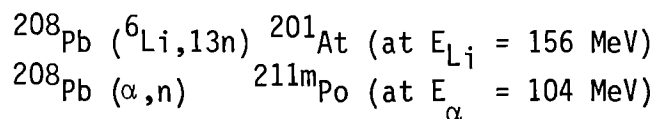

4. RESULTS

In Fig. 4, a typical alpha spectrum is shown. Some alpha lines of interest are indicated, and compiled in tab. 1.

Nuclide	Half-life	E_α	α-particles per disintegration
^{201}At	1.5 min	6.34 MeV	0.71
^{211}Bi	2.13 min	6.62	0.84
^{211}Po	0.56 sec	7.45	0.99
^{211m}Po	25.5 sec	7.27	0.91
		8.88	0.07
^{212m}Po	46 sec	11.65	0.985

Tab. 1: Decay data of observed radio nuclei (taken from Karlsruhe Nuklidkarte[24] and from ref. 14).

The method for determining the recoil energy of the product nuclei was tested by two cases of pure precompound-compound nuclear reactions of type I

$$^{208}Pb \; (^6Li,13n) \; ^{201}At \; (at \; E_{Li} = 156 \; MeV)$$
$$^{208}Pb \; (\alpha,n) \quad ^{211m}Po \; (at \; E_\alpha = 104 \; MeV)$$

The calcualted recoil energies of the compound nuclei (E_R = 4.4 MeV and E_R = 1.9 MeV, respectively) correspond to penetration depths of 220 and
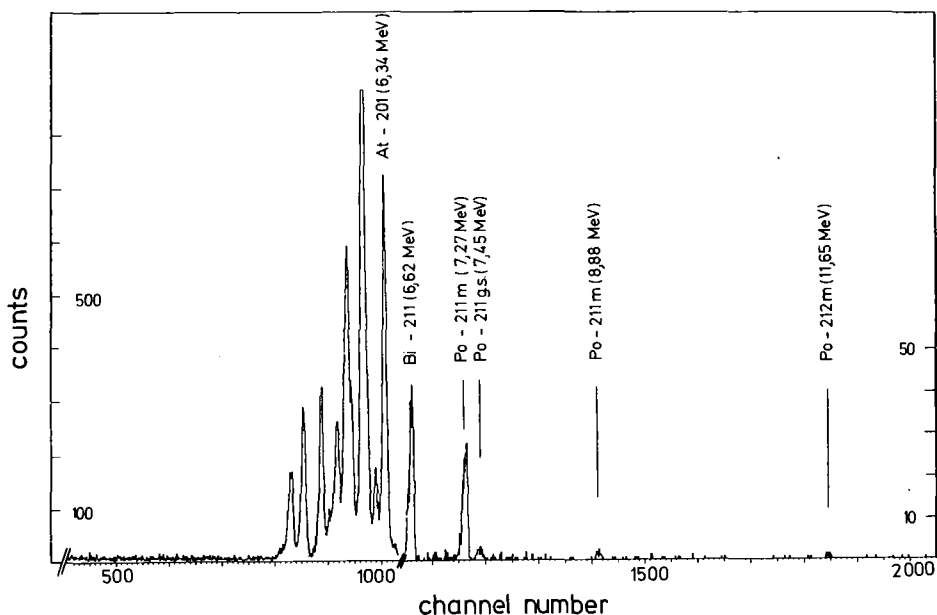
Fig. 4: Energy spectrum of alpha-particles emitted by the recoil nuclei after ^6Li bombardment of ^{208}Pb. The recoils were catched in a carbon foil (thickness ca. 20 $\mu g/cm^2$).

100 $\mu g/cm^2$ carbon[23]. Fig. 5 displays the results. The open symbols show the integral distributions of the implanted recoils from type I reactions with upper edges of the ramp at expected catcher thicknesses. For cases where both reaction paths I and II are possible (closed symbols) one immediately recognizes that the yield curves of ^6Li induced reactions follow rather closely that of the alpha particle induced reactions. A contribution of reaction type I which should appear as a second step with an upper edge at a catcher thickness of 220 $\mu g/cm^2$, is estimated to be not more than several percent of the total production cross section.

Due to energy loss the positions of the alpha lines as observed by the two detectors looking onto the front and on the backside (see fig. 3) of the catcher are found to vary with catcher thickness. Fig. 6 presents the energy loss of the ^{211m}Po alpha particles as a function of catcher thickness. Extrapolation to zero shift gives a penetration distance of the recoils of 95 ± 10 $\mu g/cm^2$ in agreement with the yield method shown in Fig. 5.
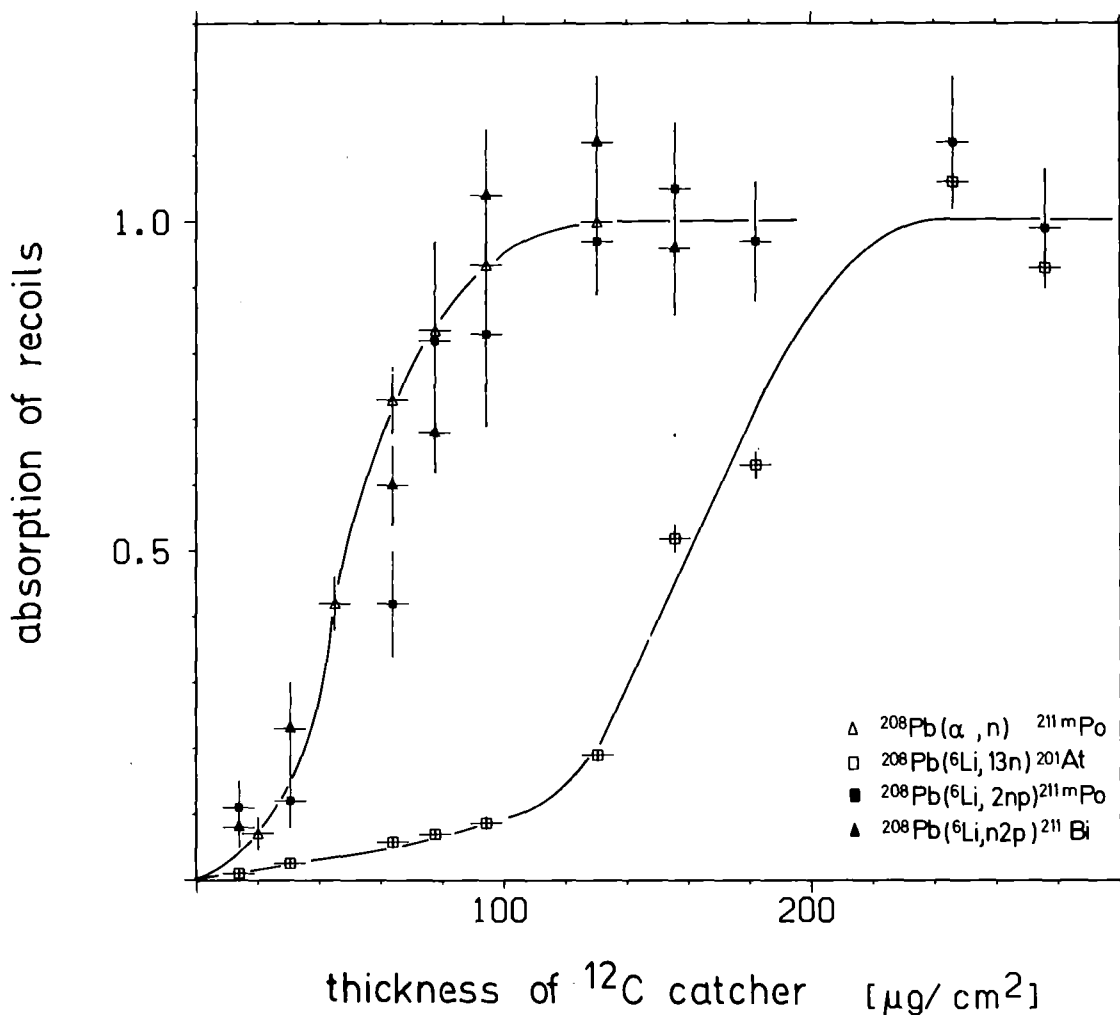
Fig. 5: Yield of recoil nuclei in carbon-catcher foils versus thickness of the foils for alpha-particle and ^{6}Li induced nuclear reactions at E_{α} = 104 MeV and E_{Li} = 156 MeV.

These results convincingly demonstrate the "internal break-up" reaction to be the prevailing mechanism. Table 2 demonstrates the remarkable agreement of the cross-sections of ^{6}Li and corresponding alpha-particle induced reactions at E_{Li} = 156 MeV and E_{α} = 104 MeV.
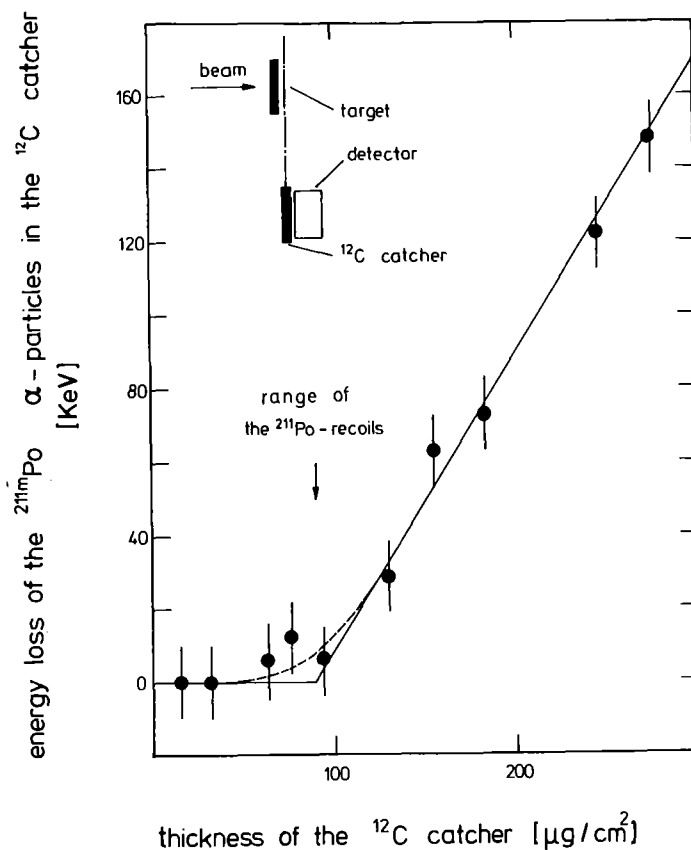
y-axis: energy loss of the ^{211m}Po α - particles in the ^{12}C catcher [KeV]

x-axis: thickness of the ^{12}C catcher [μg/cm^2]

Labels inside figure: beam, target, detector, ^{12}C catcher, range of the ^{211}Po - recoils

Fig. 6: Energy loss of the alpha-particles emitted by catched ^{211m}Po recoils and transversing varying thicknesses of the carbon catcher.

E_{Li} = 156 MeV	σ		E_{α} = 104 MeV
^{208}Pb(^{6}Li,2n+p)^{211m}Po	(85$\pm$16) μb	(82$\pm$16) μb	^{208}Pb(α,n)^{211m}Po
^{209}Bi(^{6}Li,n+2p)^{212m}Po	(43$\pm$ 8) μb	(35$\pm$ 7) μb	^{209}Bi(α,p)^{212m}Po
^{209}Bi(^{6}Li,2n+2p)^{211m}Po	(1.2$\pm$0.2)mb	(1.3$\pm$0.2)mb	^{209}Bi(α,n+p)^{211m}Po

Tab. 2 Comparison of cross-section values of corresponding reactions.

In order to check to what extent these results hold for lower bombarding energies excitation functions of ^{6}Li induced processes were measured and compared (see fig. 7) with corresponding (α,n) and (α,n+p) reactions (data taken from ref. 19). Though at lower ^{6}Li energies (<156 MeV) the "internal break-up" contribution was not experimentally separated from the compound-precompound part the very similar shape and scale of corresponding excitation functions suggest that the transfer mechanism dominates also in the lower energy part of the excitation

functions. In the case ^{208}Pb (^{6}Li,2n+p)^{211m}Pb this was qualitatively checked by analyzing the energy loss of the decay alpha-particles transversing the residual thickness of the catcher foil. Considering the shifts of the alpha-lines as function of the bombarding energy we found penetration distances which correspond to type II reaction within the experimental uncertainties.

The question arises to which extent these findings can be generalized to (^{6}Li,xn+p) reactions with x > 2, where the cross-sections are larger at projectile energies considered here. Some information may be provided by comparing corresponding excitation functions as already done for x=2 cases in fig. 7. Comparable experimental results are available for ^{197}Au from the measurements of Kropp et al.[7] and Djaloeis et al.[20]. Unfortunately, we found several indications that the measured (^{6}Li,xn+yp) cross sections may not be correct in the absolute scale as given in ref. 7. There, (^{6}Li,xn) cross sections are reported which are by factor of 6 smaller than theoretical predictions on the basis of Blann's hybrid preequilibrium model[21]. From the cross section evaluation of the present ^{208}Pb(^{6}Li,13n)^{201}At measurement we conclude that most likely the claimed discrepancy has to be reduced and that the previously reported cross sections have to be rescaled. This assumption is supported by the results of Fleissner et al.[9], even if reactions induced on different targets are compared. If we tentatively assume that the hybrid model calculations reproduce the (^{6}Li,xn) reactions correctly, a conspicuous agreement between the ^{197}Au(^{6}Li,xn+p) excitation functions (x=5, 7, 9) and the (α,(x-1)n) results[20] in the higher energy slopes above the maxima is observed when shifting the measured ^{197}Au(^{6}Li,xn+p) cross-sections by the corresponding factor. In any case (independent from the rescaling problem), there is a remarkable agreement in the ratios of (α,4n) : (α,6n) : (α,8n) and (^{6}Li,5n+p): (^{6}Li,7n+p) : (^{6}Li,9n+p) cross sections.
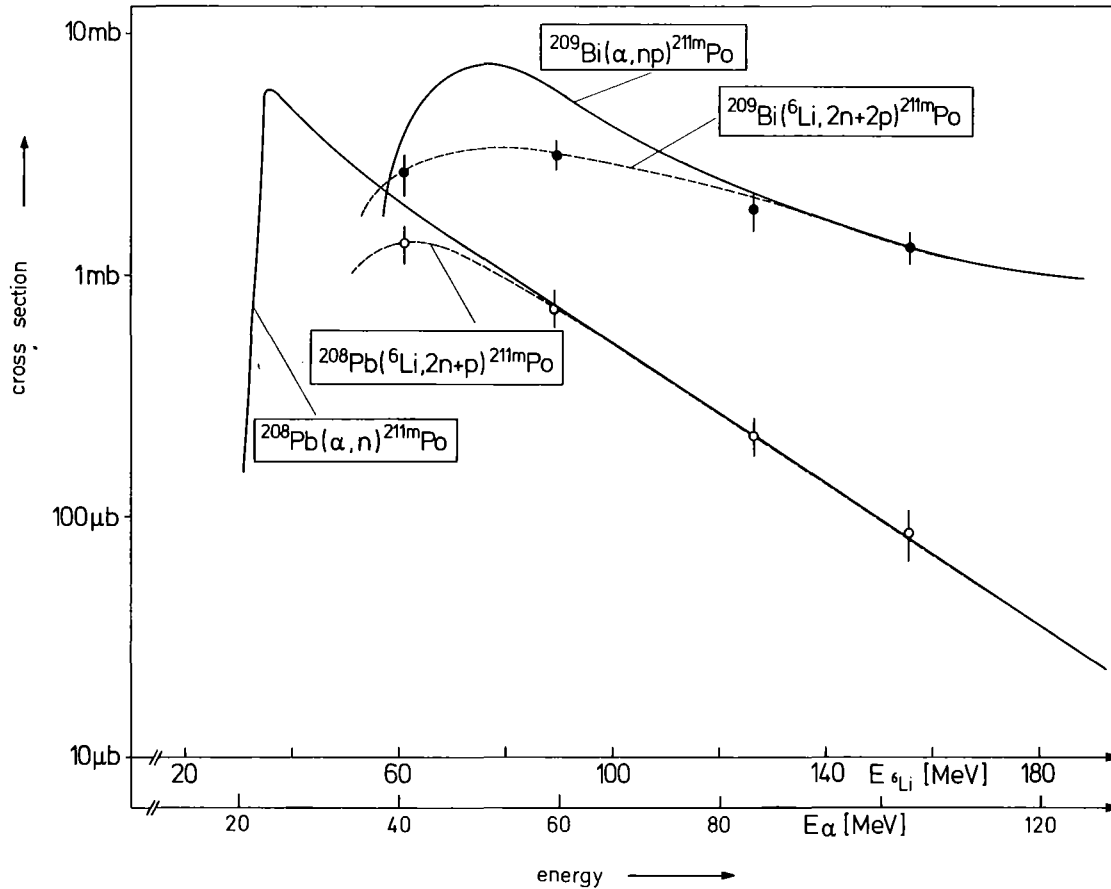
Fig. 7 Measured excitation functions for ^{6}Li induced and alpha-particle
induced reactions on ^{208}Pb and ^{209}Bi

5. CONCLUSIONS

The main result of the experiments described is the demonstration
of a relatively large contribution of transfer of beam-velocity alpha-
particles in ^{6}Li induced nuclear reactions on heavy targets. Measure-
ments of excitation functions show that (^{6}Li,xn+p) reactions behave remarkably
similar to (α,xn) processes, in particular in the high energy tails of
the excitation functions. These findings suggest that the observed transfer
reactions proceed predominantly by the precompound mechanism. There is
also evidence that the ^{209}Bi(^{6}Li,2n+2p)^{211m}Po reaction is dominated by

alpha-transfer in highly excited states and may fairly well be understood to be essentially a ^{209}Bi(α,np) process at the high energy part of the excitation function. The results confirm previous indications[7,16] and experimental findings[15,22] that cluster transfer is an important contribution in populating highly excited states in reactions with heavier projectiles. Recent break-up alpha-particle-gamma-coincidence experiments[10] with a ^{6}Li projectile energy E_{Li} = 75 MeV have also revealed the corresponding deuteron transfer in (^{6}Li,xn+p) reactions with x > 1. An explanation of the relatively large transfer probabilities of the beam-velocity alpha-particles and deuterons provides the Q-window matching[12,13] though it seems to be somewhat surprising that criteria derived for situations near the Coulomb barrier are able to account with confidence for energies far above.

ACKNOWLEDGEMENTS

REFERENCES

1) R.W. Ollerhead, C. Chasman, and D.A. Bromley, Phys. Rev. 134, 374 (1964).

2) R. Ost, E. Speth, K.O. Pfeiffer, and K. Bethge, Phys. Rev. C5, 1835 (1972).

3) R. Ost, K. Bethge, M. Gemmeke, L. Lassen, and O. Scholz, Z. Physik 266, 369 (1974).

4) D. Scholz, H. Gemmeke, L. Lassen, R. Ost, and K. Bethge, Nucl. Phys. A 288, 351 (1977).

5) H. Gemmeke, B. Deluigi, L. Lassen, and D. Scholz, Z. Physik A 286, 73 (1978).

6) B. Neumann, J. Buschmann, H.J. Gils , H. Klewe-Nebenius, H. Rebel, and S. Zagromski, to be published.

7) J. Kropp, H. Klewe-Nebenius, H. Faust, J. Buschmann, H. Rebel, H.J. Gils, and K. Wisshak, Z. Physik A 280, 61 (1977).

8) C. Castaneda, H.A. Smith, T. Ward, and T. Ness, Phys. Rev. C16, 1437 (1977).

9) J.G. Fleissner, D.A. Ratzel, F.P. Venezia, E.G. Funk, and J.W. Mihelich, Phys. Rev. C17, 1001 (1978).

10) C.M. Castaneda, H.A. Smith, jr., P.P. Singh, J. Jastrzebski, H. Karwowski, and A.K. Gaigalas, Phys. Lett. 77B, 371 (1978).

11) J. Buschmann, H.J. Gils, H. Klewe-Nebenius, Z. Majka, B. Neumann, H. Rebel, and S. Zagromski, Proceed. Intern. School of Nuclear Physics, September 1978, Predeal (Romania).
B. Neumann, J. Buschmann, H. Klewe-Nebenius, H. Rebel, and H.J. Gils, Proceed. XVII International Winter Meeting on Nuclear Physics, January 22-27, 1979, Bormio(Italy).

12) P.J.A. Buttle and L.J.B. Goldfarb, Nucl. Phys. A 176, 299 (1971) - M. Kleber and R. Beck, Phys. Lett. 43B, 98 (1973).

13) W.R. Phillips, Rep. Prog. Phys. 40, 345 (1977).

14) C.M. Lederer, J.M. Hollander, and I. Perlman, Table of Isotopes, 6th edition, 1967 John Wiley & Sons, New York, London, Sydney.
P. Hornshøj, P.G. Hansen, and B. Jonson, Nucl. Phys. A 230, 380 (1974).

15) R. Bimbot, D. Gardès, and M.F. Rivet, Nucl. Phys. A 189, 193 (1972).

16) J.L. Quebert and M. Sztark, Journ. Physique Colloq. 32, C6-255 (1971).

17) H. Münzel, J. Buschmann, G. Christaller, D. Hartmann, D. Hartwig, F. Michel, R. Schneider, and E. Schwarzbach, Nucl. Instr. $\underline{79}$, 103 (1969).

18) B. Neumann, diploma thesis, University of Heidelberg, 1976.

19) R.M. Lieder, Proceed. XVI International Winter Meeting on Nuclear Physics, January 16-21, 1978, Bormio(Italy).

20) A. Djaloeis, P. Jahn, H.-J. Probst, and C. Mayer-Böricke, Nucl. Phys. $\underline{A\ 250}$, 149 (1975).

21) B. Blann, Proceed. Int. School on Nuclear Physics, September 1974, Predeal (Romania) - Report UR-NSRL-92.
    M. Blann and F. Plasil, Program Description, private communication.

22) D.R. Zolnowski, H. Yamada, S.E. Cala, A.C. Kahler, and T.T. Sugihara, Phys. Rev. Lett. $\underline{41}$, 92 (1978).

23) L.C. Northcliffe and R.F. Schilling, Nucl. Data Tables A7 (1976).

24) W. Seelmann-Eggebert, G. Pfennig and H. Münzel, KarlsruherNuklidkarte, 4. Auflage 1974.

Appendix A: Recoil energy determination by measuring the energy
loss of alpha-particles emitted by the decaying residues

Fig. 1A shows schematically the set-up of the alpha-spectrometer
measuring the alpha-decay of the heavy nuclei residues stopped in carbon
catcher foils (see also fig. 3). The energy spectra of alpha-particles
of the decaying recoil nuclei are different for the two alpha-detectors
looking onto the front and backside of the carbon foils, respectively.
This is due to different energy losses of the alpha-particles emitted
in different directions and depends obviously on the penetration distance
of the recoils and on the catcher foil thicknesses. Considering e.g. in
fig. 2A the isolated alpha-line of ^{211m}Po (E_α = 7.27 MeV) in a spectrum
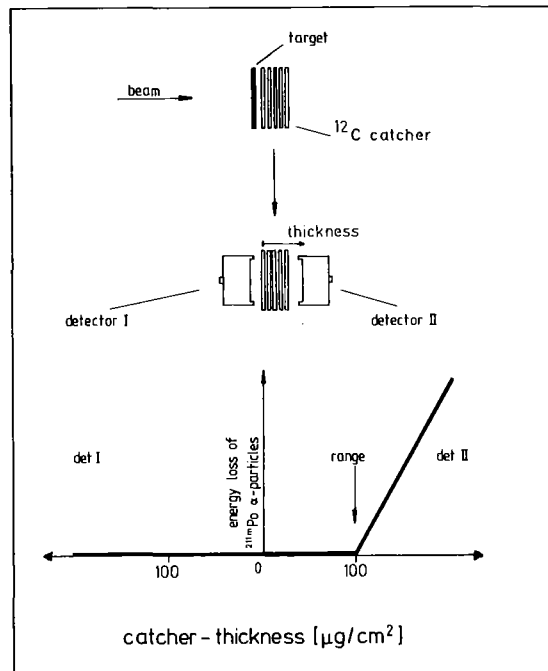taken by the backside detector II one recognizes for catcher foils, thicker

Fig. 1A: Experimental set-up for measuring the range of alpha-emitting recoils
by observing the energy loss of alpha-particles in the carbon foils.

than the maximum range, an increasing shift of the 7.27 MeV line. The
energy loss corresponding to varying catcher thicknesses is given
in fig. 6. Extrapolation to zero-shift gives the pentration distance
of the recoils (of 95 $\pm$ 10 $\mu g/cm^2$ in this case, which is in good
agreement with the yield method). As expected, in the detector I-alpha-
spectra the line position remains unshifted (fig. 3A) when increasing
the catcher thickness beyond the penetration distance since the energy
loss of the alpha-particles seen by detector I is determined by the
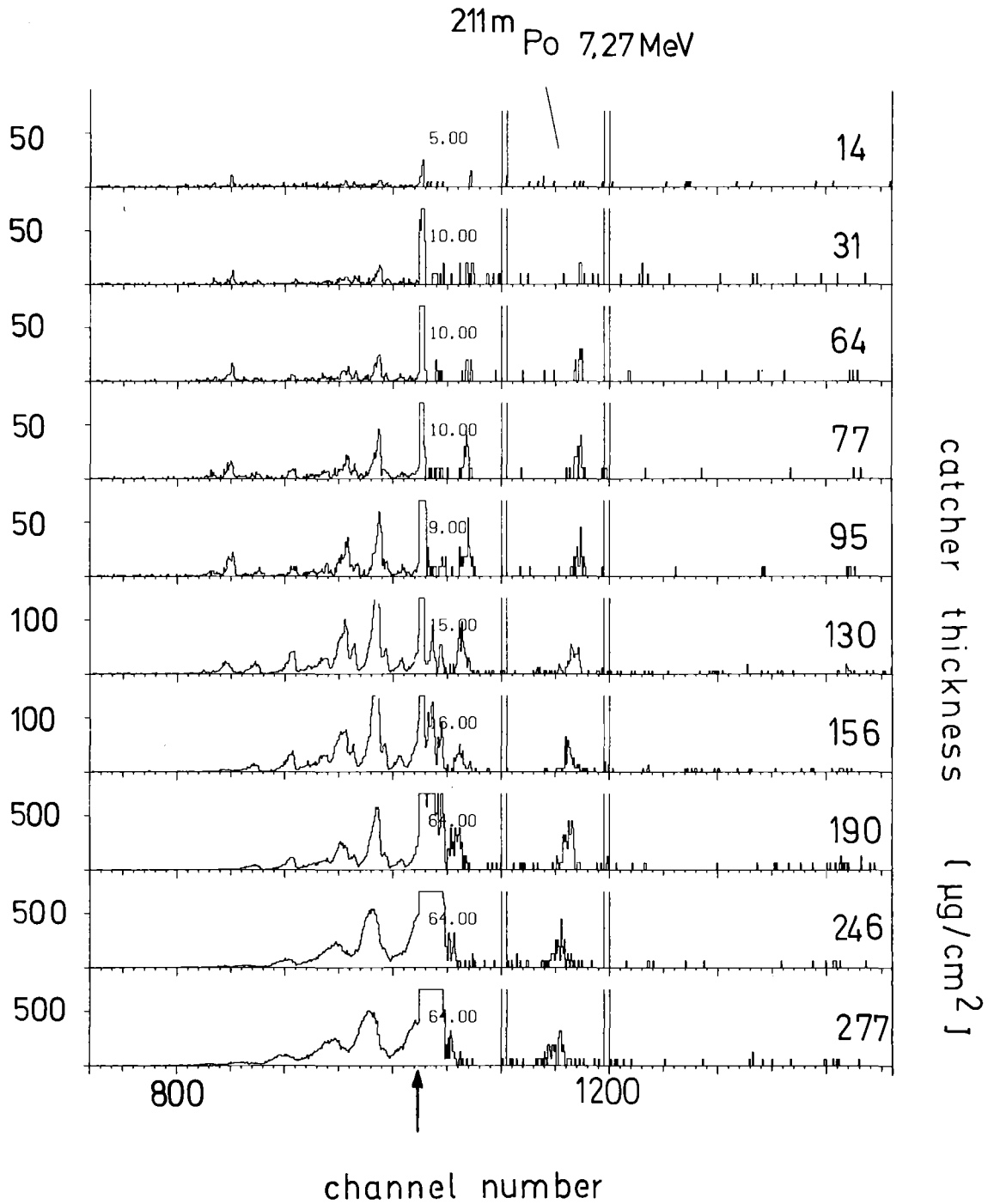range of the recoils.

Fig. 2A: Alpha-particles spectra for all used catcher foils taken by detector II. The interesting alpha-line from ^{211m}Po decay is indicated. For channel numbers above the arrow, the scale is expanded by the indicated factor.
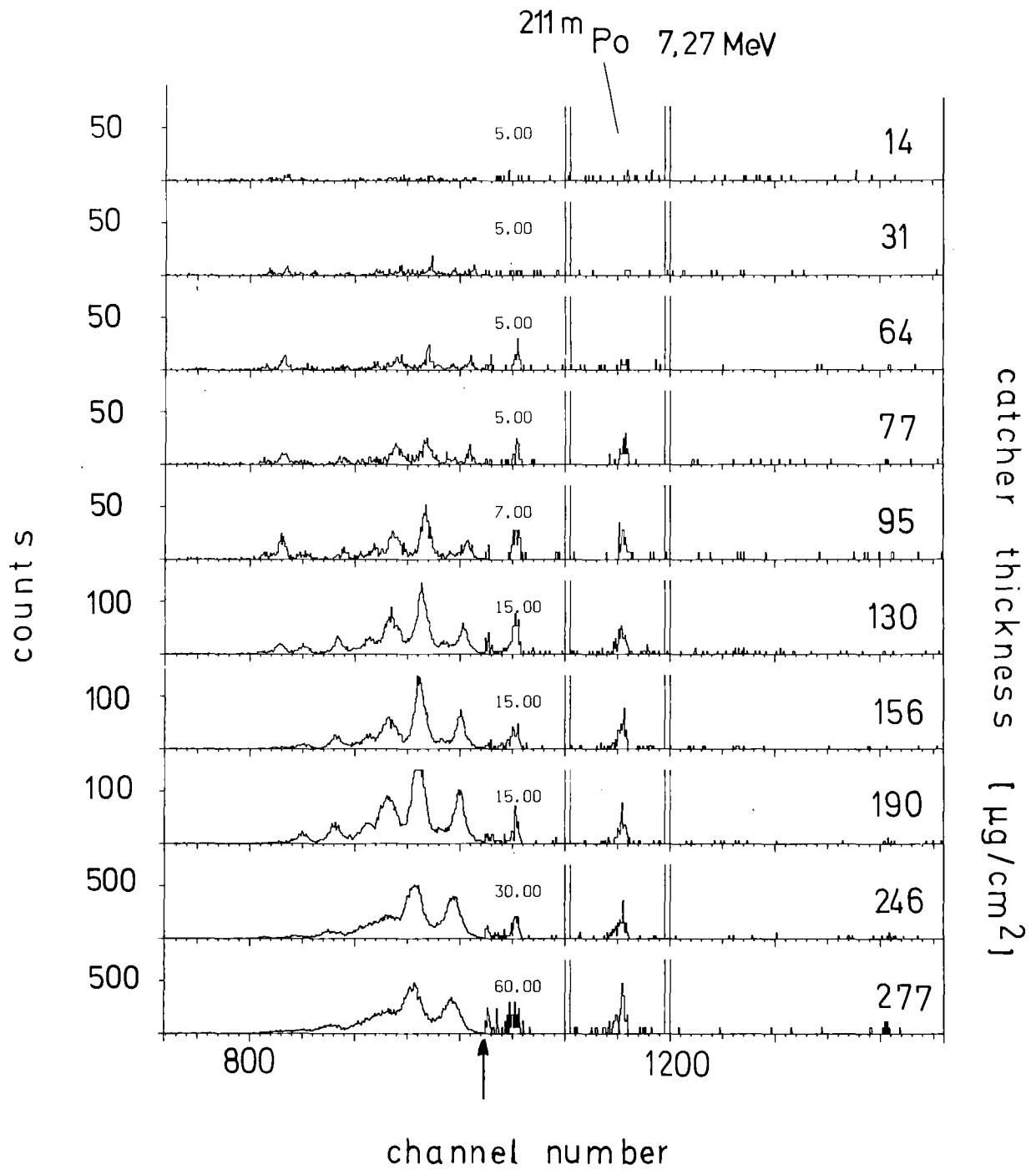
Fig. 3A: Alpha-particles spectra taken by detector I. Explanation as in fig. 2A.